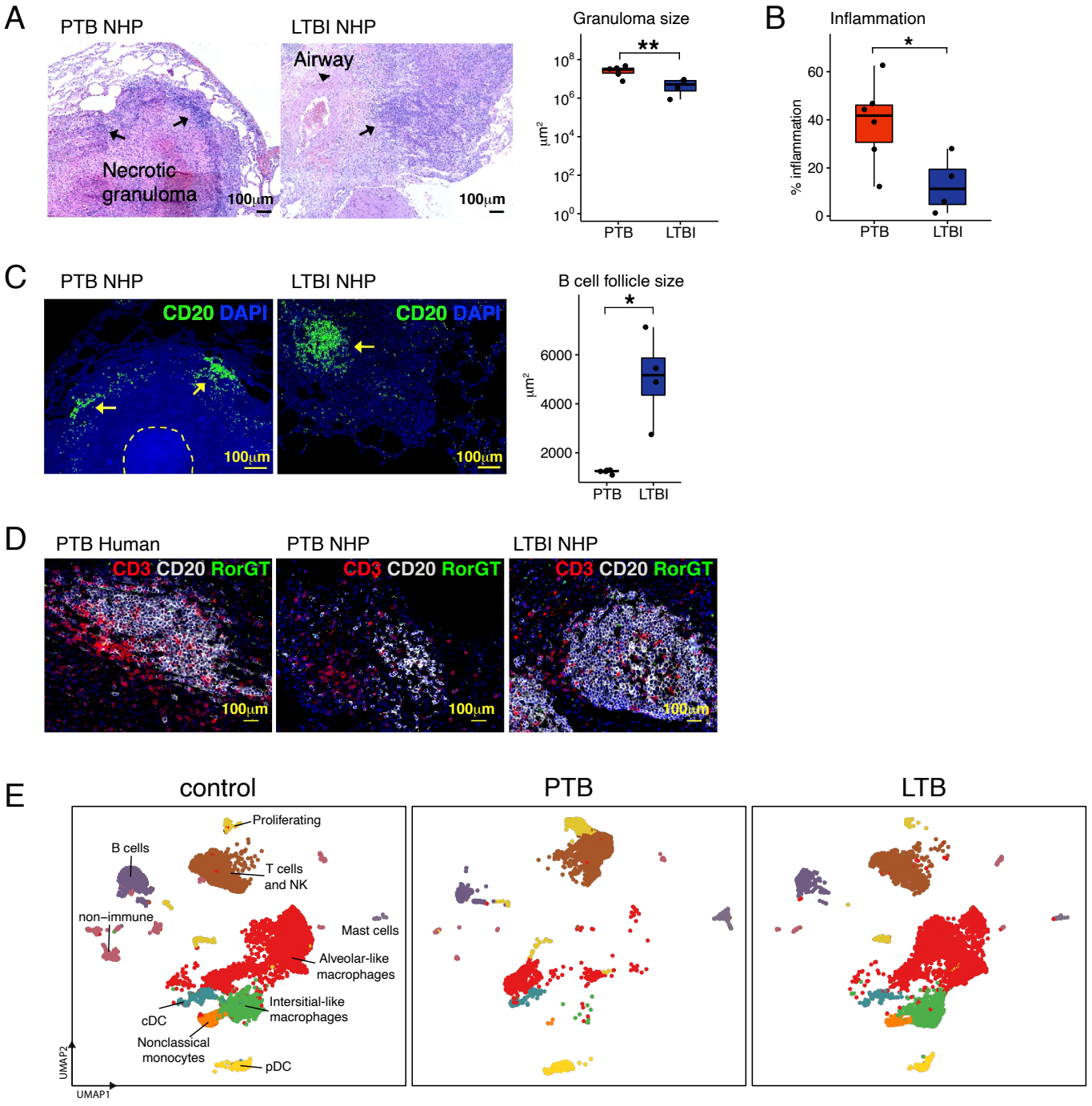

Figure S1, related to Figure 1. PTB granulomas from human and macaque display similar characteristic features.

A and **B.** Hematoxylin and Eosin staining on formalin-fixed paraffin-embedded sections from lung tissue from macaques with PTB, (n=6) and LTBI (n=4). Right panel display morphometrical quantification of the granuloma size and percentage of inflammation (B) across macaques.

C. Immunohistochemistry staining of CD20 and DAPI on formalin-fixed paraffin-embedded serial sections from macaque lung (PTB: n=6 and LTBI; n=4) as used above. Right panel display morphometrical quantification average size of B cell follicle across macaques.

D. Immunohistochemistry staining of CD3, CD20, RorγT, and DAPI on formalin-fixed paraffin-embedded sections from lung tissue from individuals with PTB, (n=6) and macaque lungs (PTB: n=6 and LTBI; n=4).

E. UMAP plots of cells from all scRNA-seq samples from macaques, split by condition and colored by the cluster. Control (n=3), LTBI (n=2) and PTB (n=5).

Data represented as mean ± SD. *$p < 0.05$, **$p < 0.01$ by Student's T test (A, B, C)

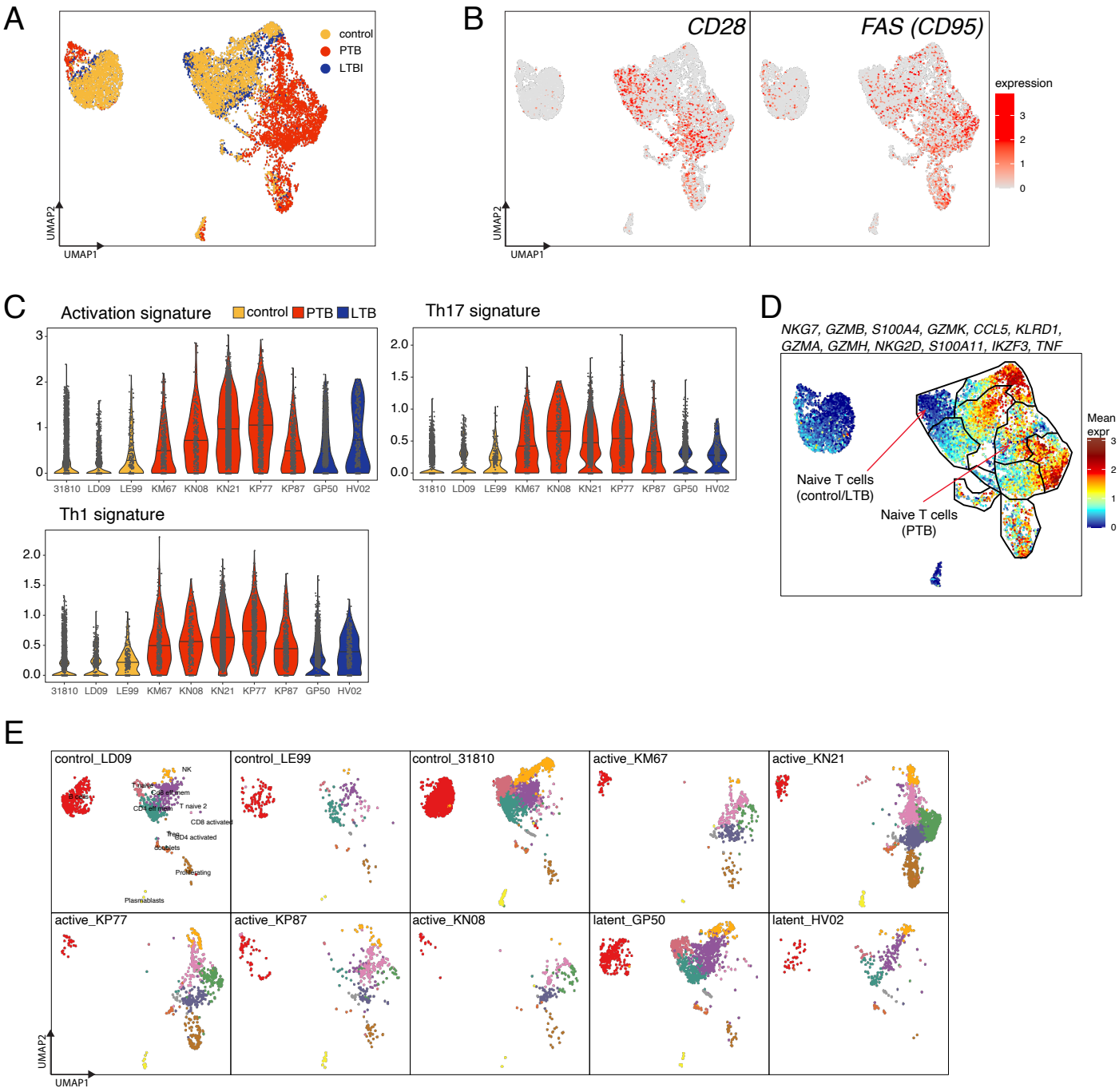

Figure S2, related to Figure 2. Disease-dependent changes in lymphoid cells by scRNA-seq for healthy macaques and macaques with PTB and LTBI.

Single cell suspensions from control (n=3), LTBI (n=2) and PTB (n=5) macaques were collected and processed for scRNA-seq as described in Fig 1.

A. UMAP plot of lymphoid cells across all samples, colored according to condition.

B. UMAP plots of CD28 and CD95 expression in lymphoid cells.

C. Violin plot of mean gene expression from Th1, Th17, and activation signatures in lymphoid cells, split by subject.

D. UMAP plot with the mean expression of genes, associated with T cell activation.

E. UMAP plots of lymphoid cells, split by sample and colored according to identified clusters.

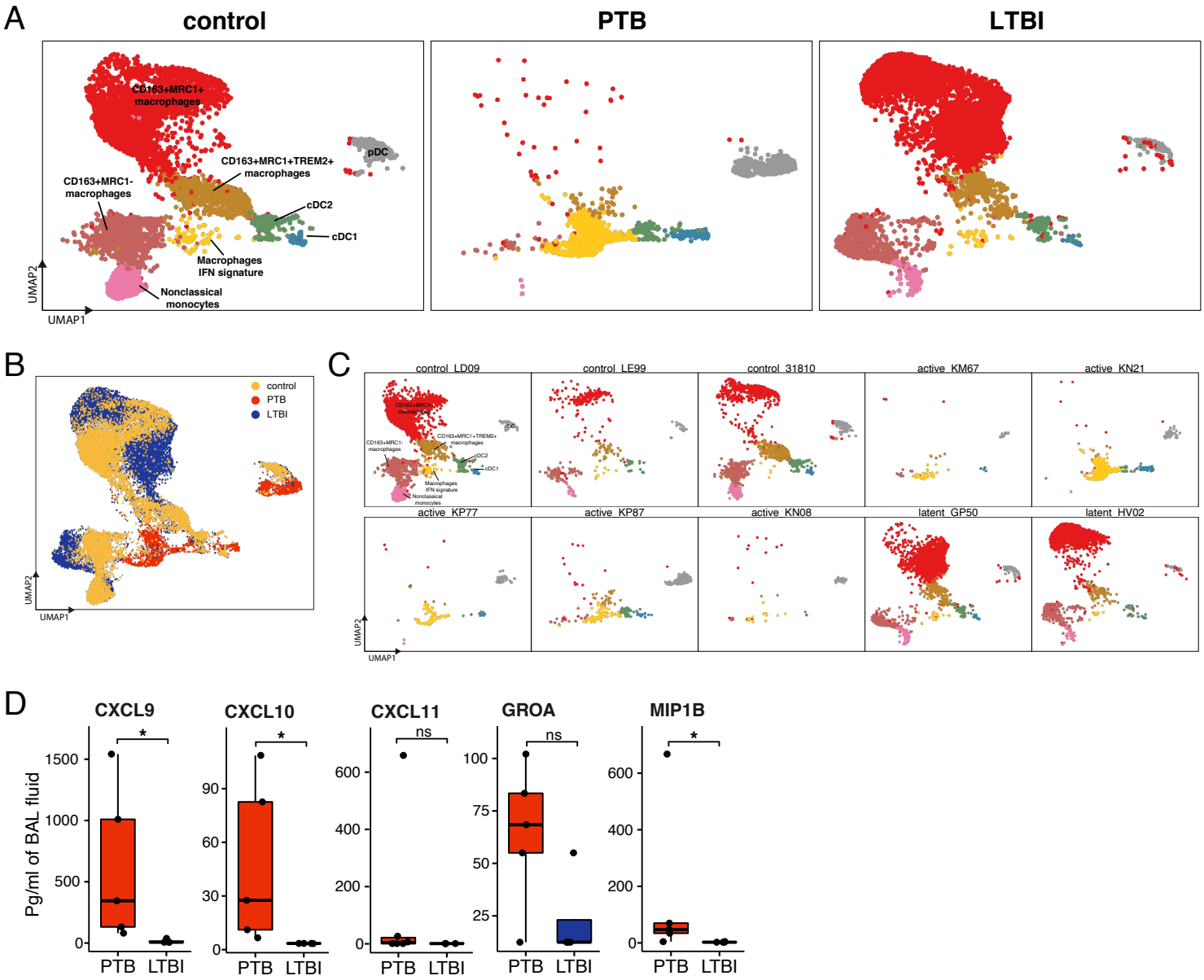

Figure S3, related to Figure 3. Disease-dependent changes in myeloid cells by scRNA-seq for healthy macaques and macaques with PTB and LTBI.

A. UMAP plots of myeloid cells split by condition and colored according to identified clusters.

B. UMAP plot of myeloid cells across all samples, colored according to condition.

C. UMAP plots of myeloid cells, split by sample and colored according to identified clusters.

D. Levels of CXCL9, CXCL10, CXCL11, CXCL-1 (GROA), and CCL-4 (MIP-1) were measured in the BAL fluid from macaques with PTB (n=5) and LTBI (n=4). Data represented as mean ± SD, NS = not significant. *p < 0.05 by Student's t-test.

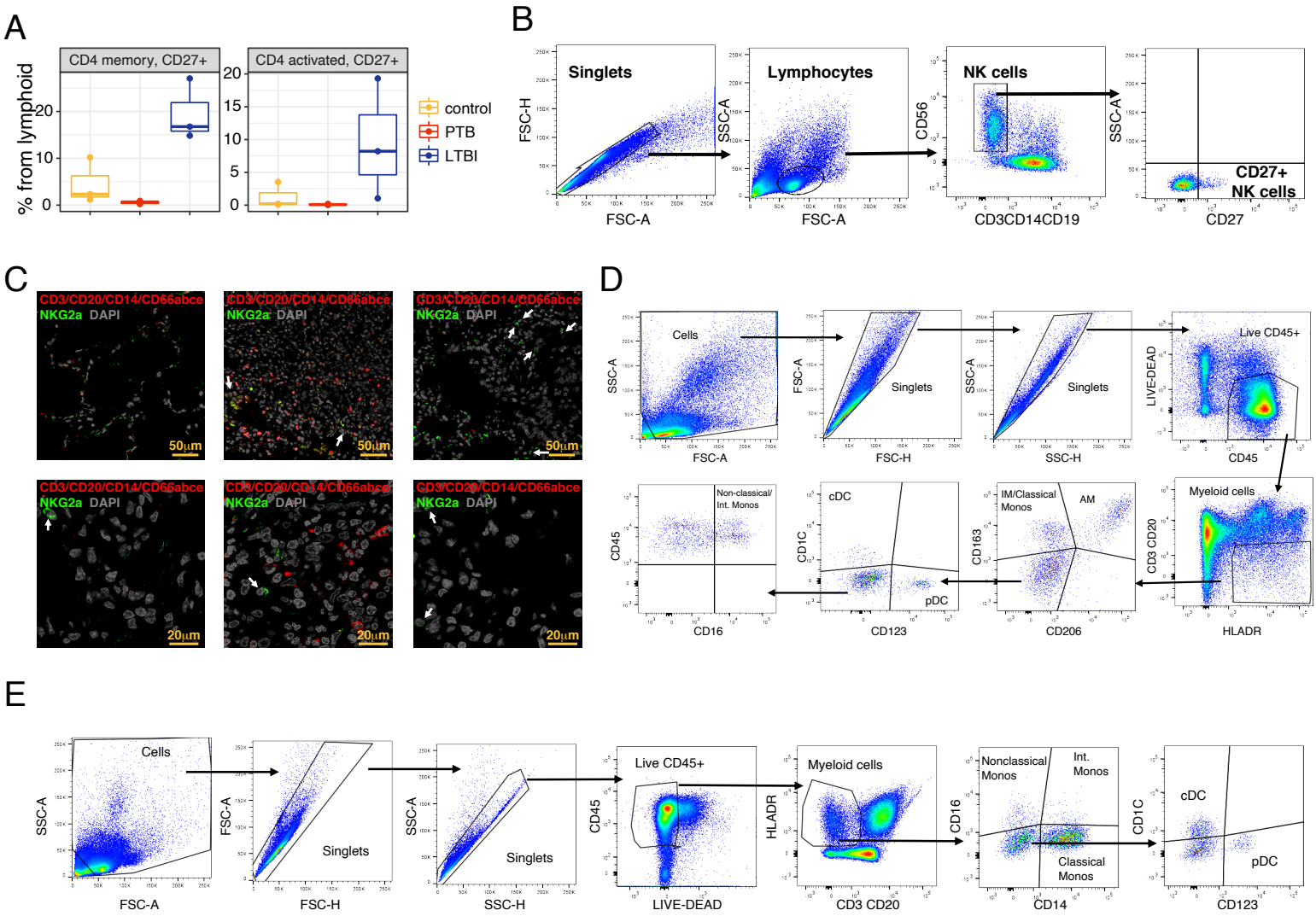

Figure S4, related to Figure 4. NK cells are increased in humans and macaques with LTBI.
for healthy macaques and macaques with PTB and LTBI.

A. Proportion of $CD4^+$ $CD27^+$ cells in two CD4 clusters from CyTOF.

B. PBMCs from healthy controls (HC, n=5) or individuals with PTB (n=25) or LTBI (n=11) were stained with CD3, CD14, CD19, CD56, and CD27 antibodies, and live populations were gated based on the following strategy: NK cells: $CD3^-CD14^-CD19^-CD56^+$ and $CD27^+$.

C. Immunohistochemistry staining of CD3, CD20, CD14, Cd66abce, NKG2a, and DAPI on formalin-fixed paraffin-embedded macaque lung (control: n=3, PTB: n=3 and LTBI; n=3). The arrowheads indicate the expected populations.

D. Lung single cell suspensions from macaques with PTB (n=9), LTBI (n=6) were stained with CD45, CD3, CD20, HLA-DR, CD206, CD163, CD16, CD1c and CD123 and the live populations were gated based on the following strategy: AMs: $CD45^+$ $CD3/CD20^-$ $HLA\text{-}DR^+$ $CD163^+$ $CD206^+$; IMs/Classical monocytes: $CD45^+$ $CD3/CD20^-$ $HLA\text{-}DR^+$ $CD163^+$ $CD206$-; Non-classical monocytes: $CD45^+$ $CD3/CD20^-$ $HLA\text{-}DR^+$ $CD163^-$ $CD206^-$ $CD16^+$ and pDC: $CD45^+$ $CD3/CD20^-$ $HLA\text{-}DR^+$ $CD163^-$ $CD206^-$ $CD1c^-$ $CD123^+$.

E. PBMC populations from the blood of individuals and macaques with PTB, LTBI and HCs were stained with CD45, CD3, CD20, HLA-DR, CD16, CD14, CD1c and CD123 and the live populations were gated based on the following strategy: Classical monocytes: $CD45^+$ $CD3/CD20^-$ $HLA\text{-}DR^+$ $CD14^+$ $CD16^-$; Non-classical monocytes: $CD45^+$ $CD3/CD20^-$ $HLA\text{-}DR^+$ $CD16^+$ $CD14^-$ or lo, intermediate monocyte: $CD45^+$ $CD3/CD20^-$ $HLA\text{-}DR^+$ $CD16^+$ $CD14^+$ and pDC: $CD45^+$ $CD3/CD20^-$ $HLA\text{-}DR^+$ $CD16^-$ $CD14^-$ $CD1c^-$ $CD123^+$.

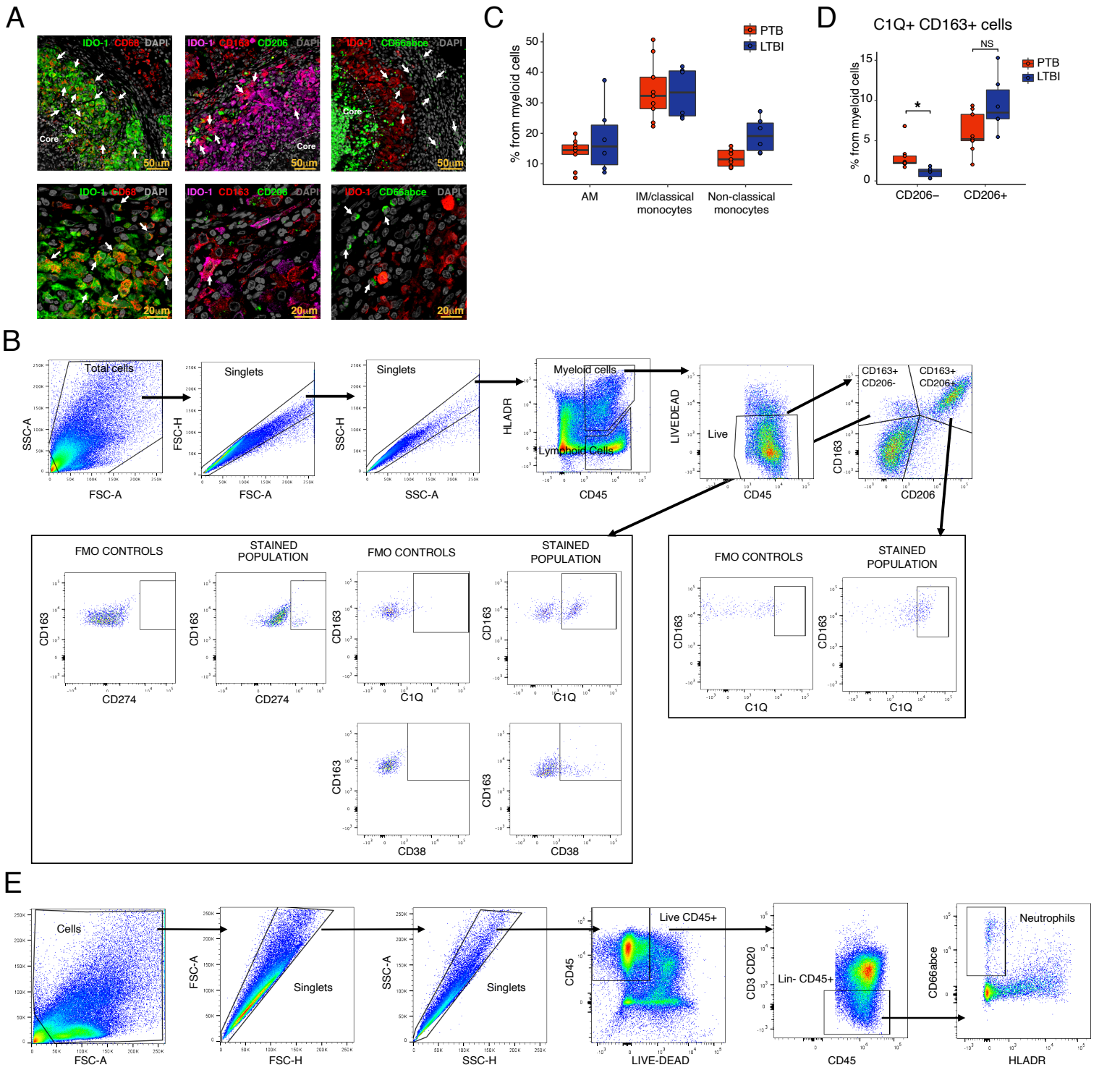

Figure S5, related to Figure 5. Lungs of macaques with PTB accumulate IFN-responsive macrophages within the rim of granulomas.

A. Immunohistochemistry staining of IDO-1, CD68; IDO-1, CD163, CD206; IDO-1, Cd66abce, and DAPI on formalin-fixed paraffin-embedded macaque lung (PTB: n=3). The arrowheads indicate the expected populations.

B. Lung single cell suspensions from macaques with PTB (n=9), LTBI (n=6) were stained with CD45, CD3, CD20, HLA-DR, CD206, CD163, CD38, CD274 and C1q and the live populations were gated based on the following strategy: $CD45^+CD3/CD20^-HLA\text{-}DR^+CD163^+CD206^-CD274^+$; $CD45^+$ $CD3/CD20^-$ $HLA\text{-}DR^+$ $CD163^+$ $CD206^-$ $CD38^+$: $CD45^+CD3/CD20\text{-}HLA\text{-}DR^+CD163^+CD206\text{-}C1Q^+$; and $CD45^+$ $CD3/CD20^-$ $HLA\text{-}DR^+$ $CD163^+$ $CD206^+$ $C1Q^+$. Fluorescence minus one (FMO) controls were used to gate the respective populations.

C-D. Percentage of AMs, IMs/classical monocytes, non-classical monocytes, $CD163^+$ $CD206^-$ $C1Q^+$, $CD163^+$ $CD206^+$ $C1Q^+$ cells were determined by flow cytometry in lung single cell suspension from PTB (n=9) and LTBI (n=6) macaques. Data represented as mean ± SD, *$p < 0.01$, by Student's t-test with Holms correction.

E. Lung single cell suspensions from macaques with PTB (n=6), LTBI (n=6) were stained with CD45, CD3, CD20, HLA-DR, CD66abce and the live populations were gated based on the following strategy: neutrophils: $CD45^+CD3/CD20^-HLA\text{-}DR^-$ $Cd66abce^+$.

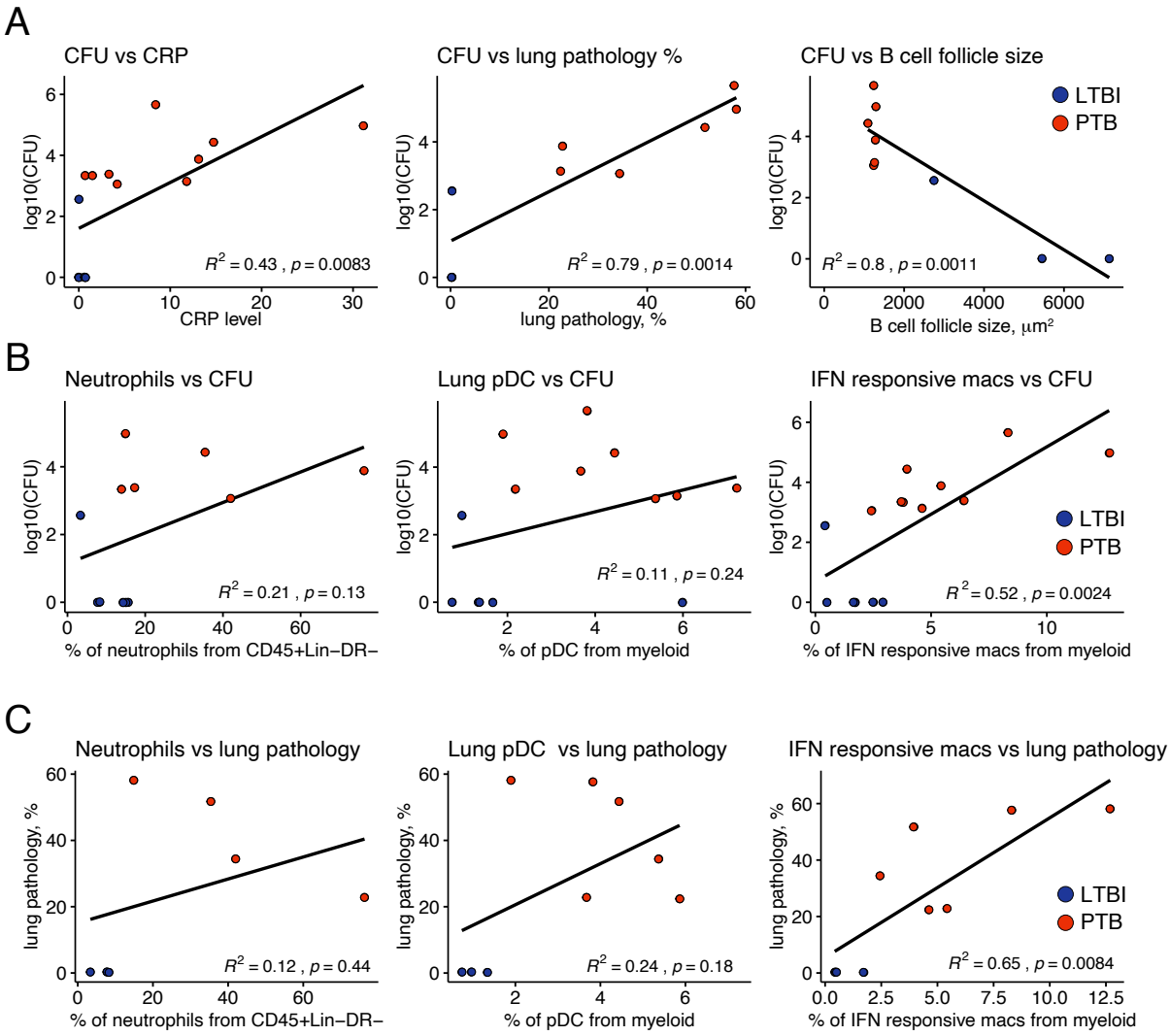

Figure S6, related to Figure 6. Accumulation of lung IFN-responsive macrophage population correlates with increased TB disease and *Mtb* burden.

A. Linear correlation between log10 of CFU identified at necropsy, and levels of CRP at necropsy, percent of lung pathology, and average area of B cell follicles measured in the lungs of macaques with PTB (red) and LTBI (blue).

B. Linear correlation between log10 of CFU at necropsy and percentage of neutrophils, pDCs, and IFN-responsive macrophage populations (as a percent of myeloid cells) measured in lungs of macaques with PTB (red) and LTBI (blue).

C. Linear correlation between the percentage of lung pathology and percentage of lung neutrophils, pDCs, and IFN-responsive macrophage populations (as a percent of myeloid cells) in the lungs of macaques with PTB (red) and LTBI (blue).

(A-C) Pearson's correlation coefficient was used.